Hydrol. Earth Syst. Sci. Discuss., 9, 3129–3163, 2012
www.hydrol-earth-syst-sci-discuss.net/9/3129/2012/
doi:10.5194/hessd-9-3129-2012

Hydrology and Earth System Sciences Discussions

Hydrochemical variability at the Upper Paraguay Basin and Pantanal wetland

A. T. Rezende Filho[1], S. Furian[2], R. L. Victoria[3], C. Mascré[4], V. Valles[4], and L. Barbiero[3,5]

[1]Universidade Federal do Mato-Grosso do Sul, Departamento de Geografia, Campus de Nova Andradina, Av. Eurico Soares Andrade 1020, 79750-000, Nova Andradina-MS, Brazil
[2]Universidade de São Paulo, Laboratório de Pedologia, Departamento de Geografia, C.P. 8105 Cep 05508-900, São Paulo, Brazil
[3]Universidade de São Paulo, Centro de Energia Nuclear na Agricultura, Laboratório de Análise Ambiental e Geoprocessamento, Av. Centenário, 303, C.P. 96, Cep 13416-000 Piracicaba-SP, Brazil
[4]Université d'Avignon et des Pays du Vaucluse, Laboratoire d'Hydrogéologie, 74 rue Louis Pasteur, 84029 Avignon Cedex 01, France
[5]Université Paul Sabatier, Géosciences Environnement Toulouse, Institut de Recherche pour le Développement, Observatoire Midi-Pyrénées, 14 Av. E. Belin, 31400 Toulouse, France

Received: 1 March 2012 – Accepted: 2 March 2012 – Published: 12 March 2012

Correspondence to: L. Barbiero (laurent.barbiero@get.obs-mip.fr)

Published by Copernicus Publications on behalf of the European Geosciences Union.

Abstract

Compartmentalization is a prerequisite to understand large wetlands that receive water from several sources. However, it faces the heterogeneity in space and time, resulting from physical, chemical and biological processes that are specific to wetlands. The Pantanal is a vast seasonally flooded continental wetland located in the centre of South America. The chemical makeup of the waters that supply the Pantanal (70 rivers) has been studied in order to establish a compartmentalization of the wetland based on soil-water interactions. A PCA-based EMMA (End-Members Mixing Analysis) procedure shows that the chemistry of the rivers can be regarded as a mixture of 3 end-members, influenced by lithology and land use, and delimiting large regions. Although the chemical composition of the end-members changed between dry and wet seasons, their spatial distribution was maintained. The results were extended to the floodplain by simple tributary mixing calculation according to the hydrographical network and to the areas of influence for each river when in overflow conditions. The resulting document highlights areas of high geochemical contrast on either side of the river Cuiaba in the north, and of the rivers Aquidauana and Abobral located in the south. The PCA-based treatment on a sampling conducted in the Nhecolândia, a large sub region of the Pantanal floodplain, allowed for the identification and prioritization of the processes that control the geochemical variability of the surface waters. Despite an enormous variability in Electrical Conductivity and pH, all data collected were in agreement with an evaporation process of the Taquari River water, which supplies the region. Evaporation and associated saline precipitations (Mg-calcite, Mg-silicates K-silicates) explained more than 77 % of the total variability in the chemistry of the regional surface water sampling.

HESSD

9, 3129–3163, 2012

1 Introduction

The upper Plata drainage system, the second largest drainage basin in South America (2.8×10^6 km^2), consists of two tributaries of similar importance: the Paraguay River, which runs with in a N–S direction, and the Paraná River, which unites at Corrientes. Over the past 30 years, the Paraná River has been increasing its annual flow (Collischonn et al., 2001). However, the relative contribution of its major tributaries is uneven given that the Paraguay River's annual discharge increase is greater than the upper Paraná's one (Pasquini and Depetris, 2010). The major difference between these tributaries is the presence of the Pantanal, at the Paraguay headwaters, which is considered as the world's largest continental wetland (0.2×10^6 km^2; Por, 1990) and exerts a discernible modulating effect (Junk and Nunes de Cunha, 2005). The Paraguay forms a natural corridor penetrating into the heart of the South American continent. To develop the region and give access to the sea, a waterway was planned from Argentina to a point upstream of Cáceres, in the brazilian Mato-Grosso. Although most research has being focused on the influences of the waterway proposed modifications on the hydrology of the Pantanal, little is known about the role of the wetland in the transfer of chemical elements across the continent.

While our knowledge on wetlands has increased significantly over the last two decades, it is still partial in many aspects (Fustec and Lefeuvre, 2000; Reddy and DeLaune, 2008). The identification, as well as the delimitation and compartmentalization give rise to problems regarding the heterogeneity in space and time that can result from the physical, chemical and biological processes prevailing in wetlands. However, this compartmentalization is a prerequisite to understand how the vast wetlands, which are supplied by several sources of water, function. The Pantanal consists of a mosaic of sub-wetlands that are usually contrasted in various aspects, i.e. hydrological, geomorphological, pedological and geochemical. Understanding the Pantanal as a whole requires the identification and distinction of compartments based on its present day functioning that could be approached through an inventory of soil-water interactions.

HESSD
9, 3129–3163, 2012

The Pantanal wetland shows curious or even contradictory features, in that although it is a large wetland under seasonal humid climate and flooded each year by numbers of rivers, the process of water concentration through evaporation was identified as a major process responsible for the geochemical variability over large areas (Barbiero et al., 2002). Therefore, methods commonly used in arid or semi-arid areas appear to be adapted to understand and describe the functioning of the Pantanal and to discriminate the processes involved (Barbiero et al., 2001, 2004). In this context, the chemical composition of rivers that supply the floodplain could control the geochemical path of water evaporation from the Pantanal, that leads to contrasting sub-regions according to the area of influence of each river (Hardie and Eugster, 1970; Valles et al., 1991). It clearly appears that ~~limentary~~ data on the hydrochemistry ~~a~~ the Upper Paraguay basin ~~is~~ lacking. The objective of this work is to identify the chemical ~~variability~~ of waters supplying the ~~depression of the~~ Pantanal, linking the water chemistry with characteristics of drained watersheds, and to explore the relationship with soil and water downriver on sub-regions of the floodplain.

2 Material and methods

2.1 The Pantanal wetlands

The Pantanal wetland is a huge and still active alluvial plain located between 15° and 22° S and 55° and 60° W (Fig. 1). The depression of the Pantanal is supplied and drained by the Paraguay River and its tributaries; most of them joining on the left bank from the Brazilian surrounding mountains and plateaus. The Northern, Eastern and Southern borders are clearly marked by the Brazilian highlands located at an altitude of about 400 to 700 m (Chapada dos Parecis, Serra das Araras, Chapada dos Guimarães, Serra São Jeronimo, Serra do Maracajú, Serra do Bodoquena). There is an opening in the north of the floodplain, through which the Paraguay River flows southward. In the south, the Paraguay River crosses a narrow area between the mountains in a region

HESSD
9, 3129–3163, 2012

called “Fecho dos Morros”, which is considered the limit of the Upper Paraguay Basin. The plain is composed of Quaternary sediments from the surrounding highlands, themselves composed of Precambrian crystalline rocks and Mesozoic sedimentary rocks.

Hot rainy summers from November to March and dry winters from April to October characterize the climate, type “Aw” according to Köppen. The average summer temperature is roughly 32 °C, while winters are dry and colder, with the possibility of occasional frost during the influx of southern polar air masses (IBGE 2003). Overall, the Pantanal has an annual water deficit of about 300 mm, resulting from an average annual rainfall of 1100 mm and an annual evapo-transpiration of 1400 mm (Alvarenga et al., 1984; Por, 1995).

The vast plain of the Pantanal provides an enormous natural control mechanism of flood waters from heavy rains during the wet period. Characterized by low slope gradients (0.3 to 0.5 m km^{-1}) and altitudes between 100 and 200 m (Assine, 2005), the plain is partially covered by seasonal floods occurring in summer (November to March). At the local level, water and solute flow are complex (Hamilton et al., 1998) and depend on many factors such as the configuration of levees, slight variations in the topography, resistance to flow related to vegetation, local rainfall intensity and tributary inputs (Girard et al., 2010). In addition to these classical factors affecting water flows in wetlands, in some parts of the Pantanal, the absence of apparent drainage networks where sub-surface stream flows are controlled by systems of thresholds between lakes (Barbiero et al., 2007, 2008). According to Hamilton et al. (1997) and on annual basis, the inflow of water in the vast system of the Pantanal is nearly equivalent to the amount drained. Thus, the water lost by evaporation is roughly balanced by direct precipitation on the floodplain.

2.2 Sampling

A total of 70 sampling points were defined to characterize the chemistry of water entering the Pantanal. Most of these points are at crossroads between the rivers and the Brazilian highways that surround the depression (Fig. 1). Geographic coordinates

HESSD
9, 3129–3163, 2012

and field measurements (pH, electrical conductivity and temperature) are given in Table 1. Samples were commonly taken from the bridge at the center of the stream, using a polyethylene sampler. Two sets of samples were taken, one during the dry season (DS) in July 2008 (including 37 samples), the other during the wet season (WS) in March 2010 (including 70 samples). To link the chemical variability within a sub-region with the type of water that supplies it, a third sampling was obtained across the plain in the heart of Nhecolândia (NH, including 74 samples), a sub-region which corresponds to the Southern part of the huge Taquari alluvial fan (Fig. 2). The sampling NH includes waters from ponds and draining fields and was conducted during the dry season along a 50 km transect located in order to intersect the ENE-WSW regional drainage, so therefore maximize chemical variability.

The electrical conductivity (EC), pH and temperature (T) were measured on aliquots. Samples were filtered (0.42 µm cellulose-acetate syringe filters) and collected in polyethylene bottles (Nalgene 125 ml) previously acid-washed, then placed at 4 °C in the dark. All samples were collected in duplicate.

2.3 Analysis

The major anions SO_4^{2-}, Cl^-, NO_3^-, NO_2^-, were analyzed by ion chromatography (Dionex DX500). The carbonate alkalinity was analyzed by carbon analyzer and HCl-titration for the most concentrated samples (Method of Gran, 1952). The major cations (Na^+, Ca^{2+}, Mg^{2+}, K^+ and silica) were analyzed by ICP and NH_4^+ by continuous flow analysis.

2.4 Data treatment

Dry season (DS) and wet season (WS) samples were subject to a discriminant analysis in order to determine the best discriminator among variables between WS and DS. Major elements were used as continuous variables and the belonging to sampling

HESSD
9, 3129–3163, 2012

DS or WS was used as qualitative variable for the discrimination. The analysis allows prioritizing discriminant functions according to their standardized coefficients.

A principal component analysis (PCA) based on the correlation matrix was carried out on major elements to identify, quantify and prioritize the factors of variability in water chemistry. The three sampling sets (DS, WS and NH) were analyzed separately. This procedure based on standardized data (n samples) centered on the mean and divided by the standard deviation, ensured that each variable (p variables) had the same weight in the PCA, regardless of the unit used.

The objective of the PCA is to calculate a lower dimensional space U defined by the eigenvectors from the PCA and to project the samples losing a minimum of information of the total variability. The dimension of the space U depends on the number of vectors (m eigenvectors) selected from the PCA. The vectors corresponding to more than 10 % of variance explained were retained.

To minimize the effect of concentration by evaporation, and to maximize the discrimination of the chemical profile of water, data from DS and WS were modified by dividing by the electrical conductivity of each sample. Thus, the PCA was performed on the variables EC and $[C^*] = [C]/\mathrm{EC}$, where $[C]$ denotes the concentrations of major elements and silica.

2.5 Mapping procedure

Considering that the DS and WS data are a mixture of end-members, a multivariate PCA-based EMMA (End-Members Mixing Analysis) procedure was conducted to identify the chemical composition of the end-members and their relative contribution in the chemistry of each sample (Christophersen and Hooper, 1992; Liu et al., 2004). The data were projected on the U space by the orthogonal projection given by:

$$U = XV^{\mathrm{T}} \quad (1)$$

where U is the $n \times m$ matrix of projected data, X is the $n \times p$ data matrix, and V is the $m \times p$ matrix of eigenvectors retained (Christophersen and Hooper, 1992). The end-

HESSD
9, 3129–3163, 2012

members were calculated independently for both DS and WS to study the variability of the end-members and samples between these two seasons. The procedure described above was applied to variables EC and [C^*] (12 variables). The proportion of each end-member in the chemistry of rivers was obtained by solving the system of equations:

$$a + b + c = 1 \quad (2)$$

$$R_{U1} = a\mathrm{EM}_{\mathrm{A\,U1}} + b\mathrm{EM}_{\mathrm{B\,U1}} + c\mathrm{EM}_{\mathrm{C\,U1}} \quad (3)$$

$$R_{U2} = a\mathrm{EM}_{\mathrm{A\,U2}} + b\mathrm{EM}_{\mathrm{B\,U2}} + c\mathrm{EM}_{\mathrm{C\,U2}} \quad (4)$$

where a, b and c are the proportions of each end-member (A, B and C) in the chemistry of the river considered, R_{U1} and R_{U2} are the coordinates of the river in the U space, $\mathrm{EM}_{\mathrm{X\,U1}}$ and $\mathrm{EM}_{\mathrm{X\,U2}}$ are the coordinates of end-member X (A, B or C) in the U space. This system of Eqs. (2)–(4) depicts a scenario of mixing with three end-members, which is the case in our study. The proportions of the end-members were used to establish a mapping of the rivers chemistry.

In a second step, the values were extended to the floodplain, based on the areas of influence of each river. The proportions of each end-member were recalculated when the waters are mixed at confluence downstream of the sampling points.

This approach is based on the results from WS sampling and on two assumptions: 1 – solutes behave conservatively during their transport and mixing of waters; 2 – water quantity increases in proportion to the drained surface area. The second point was verified in a regional report (ANA/GEF/PNUMA/OEA, 2004), where a correlation between drained area and water fluxes is established with $r^2 = 0.93$ (Fig. 3). Under these expectations, the proportion of end-members in the resulting mixture depends on their proportion in the contributory rivers, the electrical conductivity and quantity of water according to the formula:

$$x_1 \cdot \mathrm{EC}_1 \cdot q_1 + x_2 \cdot \mathrm{EC}_2 \cdot q_2 = x_3 \cdot \mathrm{EC}_3 \cdot (q_1 + q_2) \quad (5)$$

where x is the proportion of the end-member X in the chemistry of the river, EC is the electrical conductivity, q is the quantity of water. The indices 1, 2 and 3 refer to two

HESSD
9, 3129–3163, 2012

contributory rivers and to the resulting mixture, respectively. Furthermore, because of conservative mixing, we have also applied the equation:

$$EC_1 \cdot q_1 + EC_2 \cdot q_2 = EC_3(q_1 + q_2) \quad (6)$$

From Eqs. (5) and (6) we deduce:

$$x_3 = (x_1 \cdot EC_1 \cdot q_1 + x_2 \cdot EC_2 \cdot q_2)/(EC_1 \cdot q_1 + EC_2 \cdot q_2) \quad (7)$$

Water flows (q) have not been measured throughout the region. However, the relation of proportion with the drained area (s) gives:

$$x_3 = (x_1 \cdot EC_1 \cdot s_1 + x_2 \cdot EC_2 \cdot s_2)/(EC_1 \cdot s_1 + EC_2 \cdot s_2) \quad (8)$$

2.6 Concentration diagram

Water samples from NH were studied using concentration diagrams based on the sodium level, which was considered as an indicator of concentration factor of the solutions. This procedure was previously described for studies conducted in the Nhecolândia (Barbiero et al., 2008).

3 Results

3.1 Rivers hydrochemistry

The descriptive statistics of DS and WS are presented in Table 2. The electrical conductivity of water varies from 3.3 to 568 µS cm^{-1} during DS and 8.3 to 515 µS cm^{-1} during WS. Highest values were observed for rivers flowing from the Serra da Bodoquena, South of the Pantanal (Rio Salobra and Corrego Bertione, Table 1), and the lowest values were recorded from the east of the floodplain. The highest coefficients of variation were observed for NO_3^- and NH_4^+ secondary Ca^{2+}, Mg^{2+} and Cl^- in DS, and for

HESSD
9, 3129–3163, 2012

Ca^{2+}, Mg^{2+}, SO_4^{2-} and alkalinity in WS. Figure 4 shows the relationship between the conductivities in 2008 (DS) and 2010 (WS) for the 37 rivers that were not dry during sampling in 2008. Results indicate that the more dilute rivers were more concentrated in WS than in DS, whereas the waters with higher mineral charge are logically more diluted in WS. The increase in electrical conductivity of low charge waters between DS and WS is due to the increase in sulphate concentrations that average at a factor of 5, and on a factor of 9 for samples with low or medium conductivity.

The results from the discriminant analysis are presented in Table 3 and Fig. 5. A total of 96 % of the 107 WS and DS samples tested could be discriminated based on the following variable: K, NO_2 and alkalinity (DS), in opposition with SO_4 and NH_4 (WS). The discrimination is more pronounced for samples with low or medium conductivity.

Eigenvalues and eigenvectors extracted from the PCA carried out on DS and WS separately are presented in Table 4. The first factorial plan explained 66 and 62 % of the variance in DS and WS, respectively (Figs. 6 and 7). The third factorial axis, with a contribution less than 10 % of the total variance, was not considered, and it is in the plane U1-U2 that the samples and variables have been projected.

This projection provided evidence that the river waters can be regarded as a mixture from three end-members. Sample 69 from WS sampling was characterized by a peculiarly high alkalinity and high silica content (24 mg l^{-1}) and departed from the triangle defined by these three end-members. This sample, collected immediately downstream the city of Nioaque, was excluded from EMMA analysis. Among these three end-members, end-member 3 characterized the most concentrated waters and was associated with the variables alkalinity, Ca and Mg. It marked particularly the samples 57, 58, 56, 12 and 13. End-member 1 characterized diluted waters with strong influence of silica content, secondary Na^+, while being associated with different forms of nitrogen (NO_3^-, NO_2^- and NH_4^+). This end-member marked two rivers in DS (42 and 32), adding the samples 29, 31, 33, 39, 40 in WS. End-member 2 was associated with many samples without being specifically associated with one variable in 2008 (DS), whereas it is clearly associated with higher amounts of SO_4^{2-} in 2010 (WS). If the composition

HESSD
9, 3129–3163, 2012

of the end-member 3 was substantially the same in DS and WS, however that of the end-members 1 and 2 changed under the influence of higher sulphates concentrations in WS.

The results of the EMMA analysis are spatially represented on Fig. 8a (DS) and 8b (WS). Despite the change detected in the chemical composition of end-members 1 and 2 (Figs. 6 and 7), the spatial distribution of the end-members was largely similar in WS and DS samples. The strongest influence of end-member 1 was limited to two narrow regions on the eastern edge of the Pantanal. The influence of the end-member 3 marked two large portions located one in the north, from the Padre Inácio River in the west to the Cuiaba River in the east, and another one in the south from Aquidaban River in the west to Corrego Agachi in the east. Two features should be emphasized, however: (1) the percentage of influence of this end-member 3 decreased between DS and WS in the region located to the North, (2) the area of influence of this end-member increased south east of the city of Aquidauana in WS.

3.2 Influence of the river chemistry on the Pantanal floodplain

The water chemistry extended to the Pantanal floodplain, as shown in Fig. 9. Several points are worth noting. The influence of end-member 1 disappeared at the first confluence, due to the low EC (from 3 to 10 $\mu S\,cm^{-1}$) of waters involved. Thus, mainly end-members 2 and 3 had influence on the floodplain. The influence of end-member 2 dominated about 70 % of the floodplain area, covering the broad Taquari alluvial fan, the Negro River basin and the Taboco alluvial fan. In the south, the shift to the influence of end-member 3 was located along the Aquidauana River, then further west, along the Abobral River. In the north, end-member 2 also influenced the area between Correntes and São Lourenço Rivers. The shift to the compartment of the Pantanal influenced by the end-member 3 was located along Cuiaba River.

HESSD
9, 3129–3163, 2012

3.3 Chemical variability in the Nhecolândia

The descriptive statistics of the sampling NH are shown in Table 5. Cl^- and Na^+, which are generally the less controlled chemical elements, showed the highest coefficients of variation. The data set showed strong ranges of electrical conductivity ($7\,\mu S\,cm^{-1} < CE < 5820\,\mu S\,cm^{-1}$) and pH ($5.61 < pH < 10$). Despite this strong contrast, the first factorial plan (Fig. 10) explained a large percentage of the variance (77 %). The first axis (61.3 % of the variance) was significantly associated with variables EC, alkalinity, Na^+, Cl^-, SO_4^{2-}, K^+, and with the most concentrated samples (1, 74 and 75). The second axis (15.4 % of the variance) was discriminated by the variables Ca^{2+} and Mg^{2+} and associated with samples of intermediate concentration. The third axis (10.5 %, not shown) opposed two forms of nitrogen, NO_3^- and NH_4^+. This third axis was largely influenced by the chemistry of sample 54, showing a particularly high nitrate content.

The concentration diagram for NH waters (Fig. 11) indicates that pH and alkalinity increase with water mineralization. The alkalinity increases in proportion to Na^+ for Na^+ values ranging from 5 to 20 $mmol_c$, then slower for higher Na^+ concentration factors. Meanwhile, the plots representing Ca^{2+} and Mg^{2+} increase in proportion to Na^+ and then decreased significantly for the most concentrated samples. The scatter plots of Cl^- and SO_4^{2-} are widely dispersed due to their relative low concentrations. The levels of K^+ increase throughout the concentration diagram, but more slowly than sodium. The waters of the river Taquari are the most diluted samples, and are in direct continuation with the scatter plot of the waters from the Nhecolândia.

4 Discussion

The chemical variability of the rivers that supply the Pantanal wetland is controlled primarily by a lithological factor (Fig. 12). The end-member 3 is spatially associated with calcareous formations located in the north (Serra das Araras) and in the south (Serra da Bodoquena). The influence of this end-member to the east of the city of

HESSD
9, 3129–3163, 2012

Aquidauana in the rainy season should be attributed to the drainage from the basalts of the Serra Geral formation in the upper part of the Aquidauana watershed. End-members 1 and 2 are associated with sandstone formations and crystalline rocks in the eastern, north-western and the narrow southern part of the wetland. Although they were clearly discriminated on the U space (Figs. 6 and 7), the distinction between end-members 1 and 2 is more difficult to interpret, especially due to low mineral charge.

Increasing concentrations of SO_4^{2-} during the wet season is most likely the result of a different path of water. In DS, the rivers are exclusively supplied by the base flow from the sandstone formations groundwater, with very low SO_4^{2-} charge. During WS, the rivers are supplied by a large proportion of surface runoff, and the extensive monocultures of soybeans, sorghum and cotton on the surrounding plateau affect water quality. The nitrogen fertilization is in the form of ammonium sulphate, and to a lesser degree in the form of urea. This association of ammonium and sulphate is consistent with the discrimination observed between DS and WS (Table 3). Moreover, the assimilation of nitrogen as NH_4^+ is a factor of acidification of the soil solution (Valles et al., 1993), which may explain why SO_4 and NH_4 variables are in opposition to the variable alkalinity on the discriminant analysis.

The variability in water chemistry within the Nhecolândia sub-region is mainly due to the influence of evaporation. The evolution of the samples on the concentration diagrams (Fig. 11) is similar to that observed in local studies in the same region. The region is supplied by the Taquari River, which presents diluted water with a positive calcite and residual alkalinity. In these conditions and under the influence of the evaporation we observe the precipitation of calcite, with an increase in alkalinity and a decrease in calcium content (Barbiero et al., 2008). In these alkaline conditions, the magnesium appears to be also controlled and maintained at low concentration by two processes: (i) the incorporation in Mg-calcite in proportion of about 5 % to 7 % and, (ii) the formation of Mg-silicates of stevenstite and saponite types around saline lakes (Furquim et al., 2008, 2010a). Furquim et al. (2010b) suggested that the control of potassium could be

HESSD
9, 3129–3163, 2012

attributed to the formation of Fe-illite, although the thermodynamic pathways favouring illite neoformation in alkaline-saline environments have not been identified.

The plot of Cl^- and SO_4^{2-}, and in particular the scatter distribution for low charge waters, cannot be attributed to a concentration/dilution process. Instead we propose several hypotheses to explain the appearance of the scatter plots on the concentration diagram. For instance, there may be a local effect of adsorption on minerals with a R-OH structure, as it is the case of Mg-silicates according to the reaction:

$$R(Si, Mg, ...)-OH + Cl^- \rightarrow R(Si, Mg, ...)-Cl + OH^- \quad (9)$$

In the most concentrated waters, the high alkalinity prevents this reaction and Cl^- evolves conservatively in proportion to sodium. Sulphate concentrations are low and the scatter distribution in Fig. 11 could be attributed to local impact of redox processes related to the flood intensity. Barbiero et al. (2008) showed that local pedological processes have a strong influence in dissolved Cl^- and SO_4^{2-}. We should also keep in mind that the fertilization in the surrounding highland is based on $(NH_4)_2SO_4$ and KCl. Therefore, higher concentration of Cl^- and SO_4^{2-} in the floodplain could be also attributed to an effect of the upstream fertilization. It is not possible to decide between these different hypotheses solely on the basis of the major elements. An isotopic study could provide complementary information.

5 Conclusions

The chemistry of the waters that supplies the Pantanal consisted of a mixture of three end-members that depend mainly on the local lithology and land use (approximately 50 and 15 % of the total variability, respectively). The influence of land use, attributed to the presence of large crops in the edge of the Pantanal, increased during the wet season. This is probably due to a greater contribution of surface runoff that results in a considerable increase of the proportion of SO_4^{2-} and NH_4^+, and a decrease in the

HESSD
9, 3129–3163, 2012

alkalinity. Other sources of variability appeared entrenched in the geochemical background level. Despite the differences in end-member composition between wet and dry seasons (WS and DS), the spatial distribution of water chemistry highlighted the same compartments on the periphery of the Pantanal wetland.

The extension of the water chemistry by simple tributary mixing calculations showed that mainly two families of waters dominate the alluvial plain. It further revealed two areas of strong chemical contrast; one along the Cuiabá River, and the other along the Aquidauana and Abobral Rivers.

This work centers on understanding the hydrochemistry of the Upper Paraguay Basin. Future work should focus on water chemistry at the outlet of the Pantanal, located along the Paraguay River, which is the main collector of the wetland.

The gradual and continuous chemical changes from the most diluted to the most concentrated waters allowed us to link their origin to the Taquari River water. The chemical variability within the Nhecolândia can be attributed to the influence of evaporation (over 77 % of the total chemical variability) in a well-known geochemical context and already described in previous studies conducted on the local scale studies. However, one may question the strong influence of evaporation across the region, because the current climatic conditions are barely propitious for maintaining a high concentration of water that could lead to the observed salinities. Therefore, multi-scale future investigations should aim to better understand the distribution of the chemical variability in the landscape of Nhecolândia, and identify the processes responsible for this distribution.

Acknowledgement. This research was funded by FAPESP (Sao Paulo Research Foundation no. 2008/09086-7, 2008/58089-9, and 2011/12770-0) INSU-Ec2co (National Institute of Sciences of the Universe) and UFMS (Federal University of South Mato-Grosso), L. Barbiero is supported by FAPESP (no. 2009/53524-1) and CAPES (Coordination of Improvement of Higher Education Personnel) grants.

HESSD
9, 3129–3163, 2012

References

Alvarenga, S. M., Brasil, A. E., Pinheiro, R., and Kux, H. J. H.: Estudo geomorfológico aplicado à Bacia do Alto Paraguai e Pantanais Mato-grossenses, RADAMBRASIL projet, Technical Bulletin, Geomorphological Serie, 89–183, Salvador-Brazil, 1984.

ANA/GEF/PNUMA/OEA: Programa de ações estratégicas para o gerenciamento integrado do Pantanal e da bacia do Alto Paraguai, Final report, Brasilia, Brazil, 2004.

Assine, M. L.: River avulsions on the Taquari megafan, Pantanal wetland, Brazil, Geomorphology, 70, 357–371, doi:10.1016/j.geomorph.2005.02.013, 2005.

Barbiero, L., Valles, V., Régeard, A., and Cheverry, C.: Residual Alkalinity as a tracer to estimate the changes induced by a forage cultivation in a non saline sodic soil, Agric. Water Manage., 50, 229–241, doi:10.1016/S0378-3774(00)00124-4, 2001.

Barbiero, L., Queiroz Neto, J. P., Ciornei, G., Sakamoto, A., Capellari, B., Fernandes, E., and Valles, V.: Geochemistry of water and groundwater in the Nhecolândia, Pantanal of Mato Grosso, Brazil. Variability and associated processes, Wetlands, 22, 528–540, doi:10.1672/0277-5212(2002)022[0528:GOWAGW]2.0.CO;2, 2002.

Barbiero, L., Valles, V., and Cheverry, C.: Reply to the comment – some observations with respect to sodicity hazard of irrigation waters, by Van Hoorn, J. W., Agric. Water Manage. 68, 177–184, doi:10.1016/j.agwat.2004.03.011, 2004.

Barbiero, L., Furquim, S. C., Valles, V., Furian, S., Sakamoto, A., Rezende Filho, A. T., Graham, R. C., and Fort, M.: Natural arsenic in Groundwater and alkaline lakes at the Upper Paraguay Basin, Pantanal, Brazil, in: Arsenic in Soil and Groundwater Environment: Biogeochemical Interactions, edited by: Battacharya, P., Mukherjee, A. B., Bundschuh, J., Zevenhoven, R., and Loeppert, R. H., Elsevier Book Series "Trace metals and other contaminants in the environment" (J. O. Nriagu, Serie Ed.), Vol. 9, Chapt. 4, 101–126, doi:10.1016/S1875-1121(06)09004-3, Elsevier Science, Amsterdam, 2007.

Barbiero, L., Rezende Filho, A. T., Furquim, S. A. C., Furian, S., Sakamoto, A. Y., Valles, V., Graham, R. C., Fort, M., Ferreira, R. P. D., and Queiroz Neto, J. P.: Soil morphological control of hydrogeochemistry in a saline and freshwater lake landscape in the Pantanal of Nhecolândia, Brazil, Geoderma, 148, 91–106, doi:10.1016/j.geoderma.2008.09.010, 2008.

Christophersen, N. and Hooper, R. P.: Multivariate analysis of streamwater chemical data: the use of principal components analysis for the end-member mixing problem, Water Resour. Res., 28, 99–107, doi:10.1029/91WR02518, 1992.

HESSD
9, 3129–3163, 2012

Collischonn, W., Tucci, C. E. M., and Clarke, R. T.: Further evidence of changes in the hydrological regime of the River Paraguay: part of a wider phenomenon of climate change?, J. Hydrol., 245, 218–238, doi:10.1016/S0022-1694(01)00348-1, 2001.
Furquim, S. A. C., Graham, R. C., Barbiero, L., Queiroz Neto, J. P., and Valles, V.: Mineralogy and genesis of smectites in an alkaline-saline environment of Pantanal wetland, Brazil, Clays Clay Miner., 56, 579–595, doi:10.1346/CCMN.2008.0560511, 2008.
Furquim, S. A. C., Graham, R. C., Barbiero, L., Queiroz Neto, J. P., and Vidal-Torrado, P.: Soil mineral genesis and distribution in a saline lake landscape of the Pantanal wetland, Brazil, Geoderma, 154, 518–528, doi:10.1016/j.geoderma.2009.03.014, 2010a.
Furquim S. A. C., Barbiero, L., Graham, R. C., Queiroz Neto, J. P., Ferreira, R. P. D., and Furian S.: Neoformation of micas in soils surrounding an alkaline-saline lake of the Pantanal wetland, Brazil, Geoderma, 158, 331–342, doi:10.1016/j.geoderma.2010.05.015, 2010b.
Fustec, E., Lefeuvre, J. C.: Fonctions et valeurs des zones humides, Dunod, Paris, 2000.
Girard, P., Fantin-Cruz, I., Loverde de Oliveira, S. M., and Hamilton, S. K.: Small-scale spatial variation of inundation dynamics in a floodplain of the Pantanal (Brazil), Hydrobiologia, 638, 223–233, doi:10.1007/s10750-009-0046-9, 2010.
Gran, G.: Determination of the equivalence point in potentiometric titrations, Acta Chem. Scand., 4, 559–577, 1952.
Hamilton, S. K., Sippel, S. J., Calheiros, D. F., and Melack, J. M.: An anoxic event and other biogeochemical effects of the Pantanal wetland on the Paraguay River, Limnol. Oceanogr., 42, 257–272, 1997.
Hamilton, S. K., Corrêa de Souza, O., and Coutinho, M. E.: Dynamic of floodplain inundation in the alluvial fan of the Taquari River (Pantanal, Brazil), Verh. Int. Verein. Theor. Angew. Limnol., 26, 916–922, 1998.
Hardie, L. A. and Eugster, H. P.: The evolution of closed-basin brines, Miner. Soc. Am. Spec. Pap., 3, 273–290, 1970.
IBGE: Base cartográfica integrada digital do Brasil ao milionésimo: versão 1.0 para ArcGis Desktop-ArcView, IBGE CD-Rom, Rio de Janeiro, Brazil, 2003.
Junk, W. J. and da Cunha, C. N.: Pantanal: a large South American wetland at a crossroads, Ecol. Engin., 24, 391–401, doi:10.1016/j.ecoleng.2004.11.012, 2005.
Liu, F., Williams, M., and Caine, N.: Source waters and flowpaths in a seasonally snow-covered catchment, Colorado Front Range, USA, Water Resour. Res., 40, W09401, doi:10.1029/2004WR003076, 2004.

HESSD
9, 3129–3163, 2012

Pasquini, A. and Depetris, P. J.: ENSO-triggered exceptional flooding in the Parana River: Where is the excess water coming from?, J. Hydrol., 383, 186–193, doi:10.1016/j.jhydrol.2009.12.035, 2010.
Por, F. D.: The Pantanal of Mato Grosso (Brazil): World's Largest Wetlands, Monographiae Biologicae, Springer, 1995.
Reddy, K. R. and DeLaune, R. D.: Biogeochemistry of wetlands: Science and applications, CRC Press Inc, Boca Raton, USA, 2008.
Rezende Filho, A. T.: Variabilidade química das águas na Bacia do Alto Paraguai: Uma compartimentação do Pantanal Mato-grossense, Ph.D., University of Sao Paulo, São Paulo, Brazil, 152 pp., 2011.
Valles, V., Pachepsky, Y. A., and Ponizovsky, A. A.: Invariant criteria for irrigation water quality assesment in arid and semi arid regions, in: Genesis and control of fertility of salt affected soils. ISSS Subcommission on salt affected soils Science, USSR, V. V. DOKUCHAEV Soil Institute, Moscow, 330–333, 1991.
Valles, V., Lefevre, A. M., and Ponizovsky, A. A.: Alkalization of nutrient solutions by sorghum, Commun. Soil Sci. Plant Anal., 24, 379–388, doi:10.1080/00103629309368808, 1993.

HESSD
9, 3129–3163, 2012

Table 1. Field measurements and coordinates of DS and WS samplings.

Sample point	River name	*X* coord UTM (m)	*Y* coord UTM (m)	DS 2008 EC ($\mu S\,cm^{-1}$)	WS 2010 EC ($\mu S\,cm^{-1}$)	DS 2008 pH	WS 2010 pH
1	Cuibá	591 992	8 278 978	84	175	7.68	7.19
2	Bento Gomes	555 756	8 231 155	188	110	7.62	7.36
3	Maneta I	561 608	8 184 171	–	32.2	–	6.19
4	Boca do Vale	565 022	8 175 578	–	72.4	–	6.55
5	Cuibá	566 337	8 173 770	74	70.9	7.47	6.54
6	Bento Gomes	548 710	8 196 169	–	74.9	–	6.62
7	Das Trairas	538 175	8 222 180	108	103	7.43	7.16
8	Formiga	517 540	8 230 031	335	218	7.6	7.55
9	Figueira	508 275	8 233 985	297.4	212	7.47	7.33
10	*unnamed*	508 141	8 234 616	–	150	–	7.46
11	Dos Macacos	502 847	8 238 699	–	75.4	–	7.05
12	Córrego Sangradouro	488 769	8 237 437	354	62	8.18	6.8
13	Córrego Sangradorzinho	486 839	8 238 410	505	67	8.01	6.92
14	Das Flexas	471 355	8 225 208	262	100	8.13	7.35
15	Paraguai	424 761	8 222 717	44	49	6.95	6.4
16	Padre Inácio	410 123	8 223 775	320	188.5	7.33	7.14
17	Jaurú	391 309	8 214 515	59.2	115.6	7.5	6.83
18	Aricá	618 670	8 264 051	–	35.1	–	6.62
19	*unnamed*	643 214	8 259 231	–	50.4	–	7.12
20	Aricá Mirim	643 986	8 256 529	–	27.1	–	6.76
21	Córrego do Cervo	644 011	8 252 503	47.9	41.2	6.8	6.65
22	Aguas Quentes	659 092	8 243 162	27.8	31.4	6.64	6.96
22*	Aguas Quentes hot spring	659 092	8 243 162	65.2	69.1	6	5.75
23	São Lourenço	722 310	8 230 205	18.17	38	6.97	7.02
24	Areial	725 672	8 225 462	–	44.3	–	6.94
25	Tugoré	737 175	8 207 253	–	51.5	–	7.03
26	Vermelho	768 431	8 177 496	26.5	39	7.2	7.02
27	Inhumas	744 340	8 134 806	–	15.3	–	5.23
28	Ponte de Pedra	738 269	8 116 883	–	13.6	–	5.69
29	Cachoeira	738 334	8 105 777	–	11.8	–	5.33
30	Itiquira	737 941	8 091 244	16.18	24.8	6.7	6.99
31	Sozinho	737 773	8 085 673	–	10.2	–	5.75
32	Correntes	739 894	8 061 356	5.05	10.8	6.38	6.05
33	Benjamin	737 791	8 038 055	–	10.1	–	5.59
34	Piquiri	744 750	8 017 762	17.3	27.3	6.81	6.6
35	Claro	748 376	7 986 646	–	32	–	6.55
36	Claro	745 182	7 963 080	–	17.5	–	6.22
37	Taquarí	738 629	7 950 094	17.6	29.2	6.9	6.95
38	Coxim	737 903	7 947 151	32	33	6.8	6.7
39	Riacho Claro	728 939	7 923 208	–	8.7	–	5.61
40	Córrego Fundo	730 344	7 916 226	–	8.7	–	5.55
41	Verde (Highway)	727 168	7 909 208	–	16.4	–	6.09
42	Verde	720 637	7 904 625	3.55	8.3	5.5	5.48
43	Negrinho	719 870	7 890 980	–	43.7	–	6.78
44	*unnamed*	718 384	7 882 929	–	55.3	–	7.32
45	Córrego Mumbuca	718 067	7 877 005	17.1	21.5	6.5	6.38
46	Córrego Garimpo	710 840	7 857 975	–	52.4	–	6.81
47	Negro	691 628	7 862 831	33.7	36.2	6.92	6.66
48	Taboco	641 526	7 780 008	19.53	44.9	6.71	6.49
49	Dois Irmãos	648 429	7 728 861	–	114.9	–	7.85
50	Cachoeirão	680 237	7 735 017	–	121	–	7.61
51	Aquidauana	653 171	7 734 398	74.6	78.8	7.59	7.53
52	Taquarussú	627 188	7 732 732	–	75.1	–	7.18
53	Córrego Acogô	620 001	7 732 233	36.5	42.5	6.75	6.75
54	Córrego Laranjal	599 105	7 741 379	–	134	–	7.56
55	Córrego Agachi	588 936	7 749 514	200	203	7.44	7.77
56	Miranda	562 568	7 761 352	249	181	7.97	7.39
57	Salobra	544 374	7 763 661	568	459	7.75	7.64
58	Córrego Bertione	535 998	7 718 894	–	515	–	7.80
59	Córrego Igrejinha	509 329	7 670 101	–	222	–	8.23
60	Córrego Catitú	494 183	7 672 968	–	55.5	–	7.39
61	Aquidabã	472 150	7 695 152	245	175.1	7.4	7.75
62	Naitaka	439 952	7 718 740	144.3	103.3	6.76	6.8
63	Nabileque	434 088	7 716 911	–	106	–	6.95
64	Branco	455 872	7 651 866	77.8	99.2	7.35	7.38
65	Tereré	461 640	7 632 796	131.5	68.2	8.54	7.72
66	Amonguijá	465 962	7 610 405	92.2	56.7	7.73	7.65
67	São Lourenço	471 392	7 603 639	–	69.3	–	7.59
68	Paraguay – Porto Murtinho	408 505	7 600 872	–	91.4	–	6.91
69	Nioaque	621 074	7 661 114	155	167	7.69	7.91

HESSD
9, 3129–3163, 2012

Table 2. Descriptive statistics of major elements in sampling DS (dry season 2008) and WS (wet season 2010).

	Unit	Minimum	Maximum	Mean value	Variance v	Standard deviation	Coefficient of variation
			Dry season 2008 – 37 samples				
EC	$\mu S\,cm^{-1}$	3.55	568	134	20405	143	1.07
pH	–	5.50	8.5	7.22	0.4	0.62	0.09
Ca^{2+}	$mmol\,l^{-1}$	5×10^{-3}	2.2	0.34	0.22	0.47	**1.40**
K^{+}	$mmol\,l^{-1}$	5×10^{-3}	0.2	0.057	1.7×10^{-3}	0.04	0.72
Mg^{2+}	$mmol\,l^{-1}$	4×10^{-4}	1.5	0.28	0.15	0.38	**1.39**
Na^{+}	$mmol\,l^{-1}$	0.01	0.6	0.14	0.02	0.15	1.04
Si	$mg\,l^{-1}$	4.3	17.0	8.9	13.6	3.68	0.41
Cl^{-}	$mmol\,l^{-1}$	5×10^{-3}	0.28	0.033	0.002	0.045	**1.37**
NO_2^{-}	$mmol\,l^{-1}$	nd	0.048	0.006	10^{-4}	0.012	**1.87**
SO_4^{2-}	$mmol\,l^{-1}$	nd	0.059	0.009	10^{-4}	0.01	1.16
NO_3^{-}	$mmol\,l^{-1}$	nd	0.025	0.005	4×10^{-5}	0.006	1.09
NH_4^{+}	$mmol\,l^{-1}$	nd	0.014	0.002	10^{-5}	0.003	**1.40**
Alk.	$mmol_c$	9×10^{-3}	6.9	1.36	2.8	1.68	1.23
			Wet season 2010 – 69 samples				
EC	$\mu S\,cm^{-1}$	8.3	515	86	7932	89	1.04
pH	–	5.23	8.23	6.87	0.47	0.69	0.10
Ca^{2+}	$mmol\,l^{-1}$	4.2×10^{-3}	3.29	0.34	0.32	0.57	**1.68**
K^{+}	$mmol\,l^{-1}$	5.5×10^{-3}	0.07	0.0211	0.0002	0.013	0.61
Mg^{2+}	$mmol\,l^{-1}$	4×10^{-4}	2.27	0.2348	0.1151	0.34	**1.45**
Na^{+}	$mmol\,l^{-1}$	1.34×10^{-2}	0.28	0.0618	0.0029	0.054	0.87
Si	$mg\,l^{-1}$	2.9	23.3	6.87	15.12	3.89	0.57
Cl^{-}	$mmol\,l^{-1}$	2×10^{-3}	0.18	0.0318	0.0008	0.029	0.91
NO_2^{-}	$mmol\,l^{-1}$	nd	0.014	0.001	4.53×10^{-6}	0.002	**1.61**
SO_4^{2-}	$mmol\,l^{-1}$	4.2×10^{-3}	0.33	0.046	0.003	0.059	1.27
NO_3^{-}	$mmol\,l^{-1}$	nd	0.047	0.0069	5.2×10^{-5}	0.007	1.22
NH_4^{+}	$mmol\,l^{-1}$	nd	0.029	0.016	9.2×10^{-5}	0.01	0.61
Alk	$mmol_c$	0.009	5.414	0.573	0.799	0.89	**1.56**

HESSD
9, 3129–3163, 2012

Table 3. Results of the discriminant analysis based on major elements and carried out on samplings DS and WS.

Observed/predicted	DS	WS	Total	% correct
DS	36	1	37	97.3 %
WS	3	67	70	95.71 %
Total	39	68	107	96.26 %

HESSD
9, 3129–3163, 2012

Table 4. Results of the PCA carried out on samplings DS and WS.

	DS – Dry Season 2008		WS – Wet Season 2010	
Factorial axis	Eigenvalue	% of var.	Eigenvalue	% of var.
1	6.77	52.05	6.04	46.476
2	1.83	14.08	2.02	15.519
3	1.23	9.46	1.24	9.525

HESSD
9, 3129–3163, 2012

Table 5. Descriptive statistics of major elements in sampling NH (Nhecolândia).

	Unit	Minimum	Maximum	Mean value	Variance v	Standard deviation	Coefficient of variation
EC	$mS\,cm^{-1}$	0.007	5.82	0.41	0.996	0.998	2.43
Cl^-	$mmol\,l^{-1}$	0.011	5.87	0.29	0.826	0.909	3.16
SO_4^{2-}	$mmol\,l^{-1}$	0.003	0.88	0.064	0.016	0.125	1.93
NO_3^-	$mmol\,l^{-1}$	nd	0.72	0.033	0.008	0.092	2.82
NH_4^+	$mmol\,l^{-1}$	nd	0.07	0.009	0.0002	0.017	1.91
Ca^{2+}	$mmol\,l^{-1}$	0.013	1.26	0.22	0.060	0.246	1.11
Mg^{2+}	$mmol\,l^{-1}$	0.012	1.36	0.19	0.052	0.228	1.23
Na^+	$mmol\,l^{-1}$	0.027	43.10	2.41	52.22	7.228	2.99
K^+	$mmol\,l^{-1}$	0.034	8.14	0.87	2.26	1.504	1.74
Alk	$mmol_c$	0.102	49.44	3.68	64.02	8.002	2.18

HESSD
9, 3129–3163, 2012

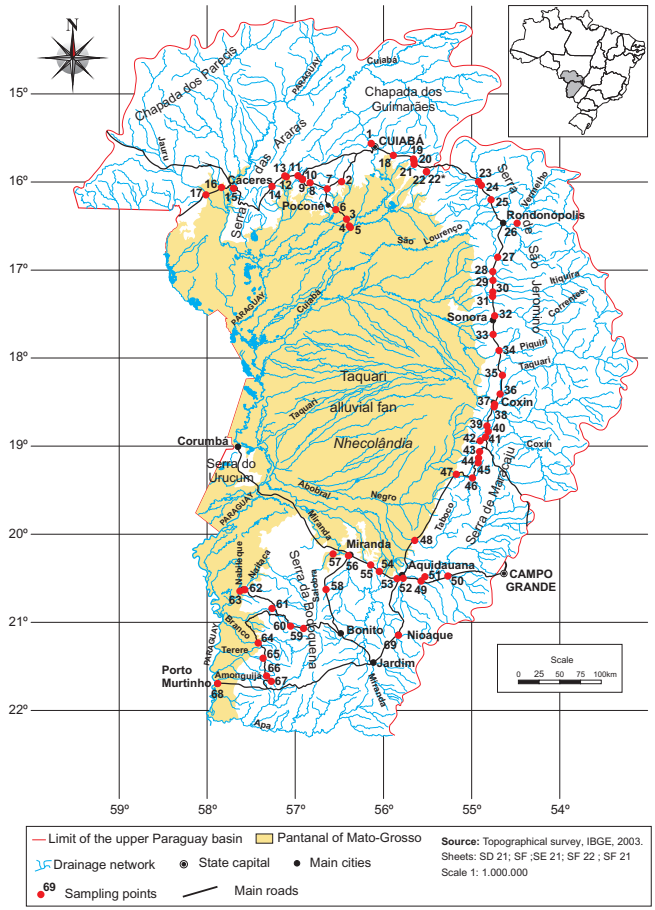

Fig. 1. The Upper Paraguay Basin, the Pantanal wetland and the Nhecolândia sub-region. Location of the sampling points DS and WS.

HESSD
9, 3129–3163, 2012

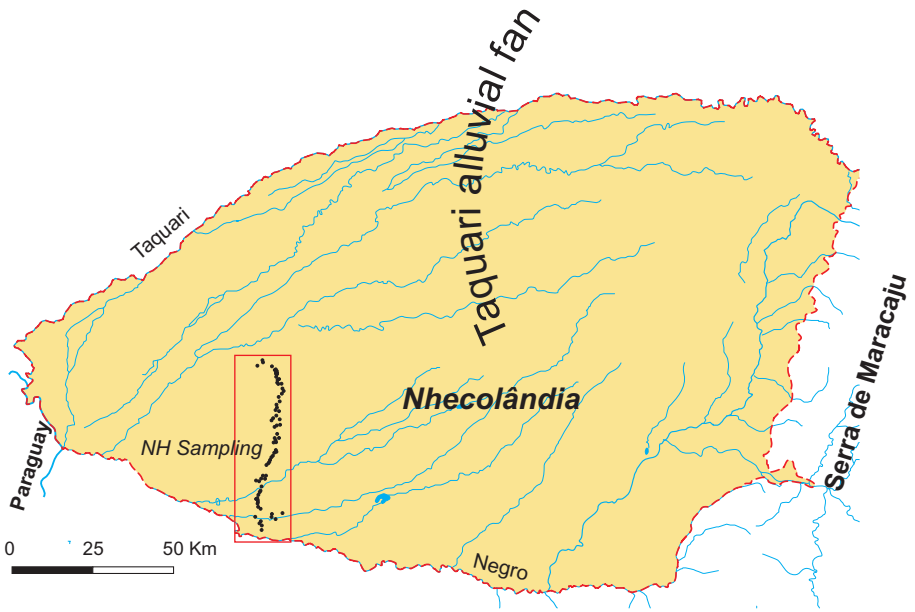

Fig. 2. Location of the sampling NH in the Nhecolândia, southern part of the Taquari alluvial fan.

HESSD
9, 3129–3163, 2012

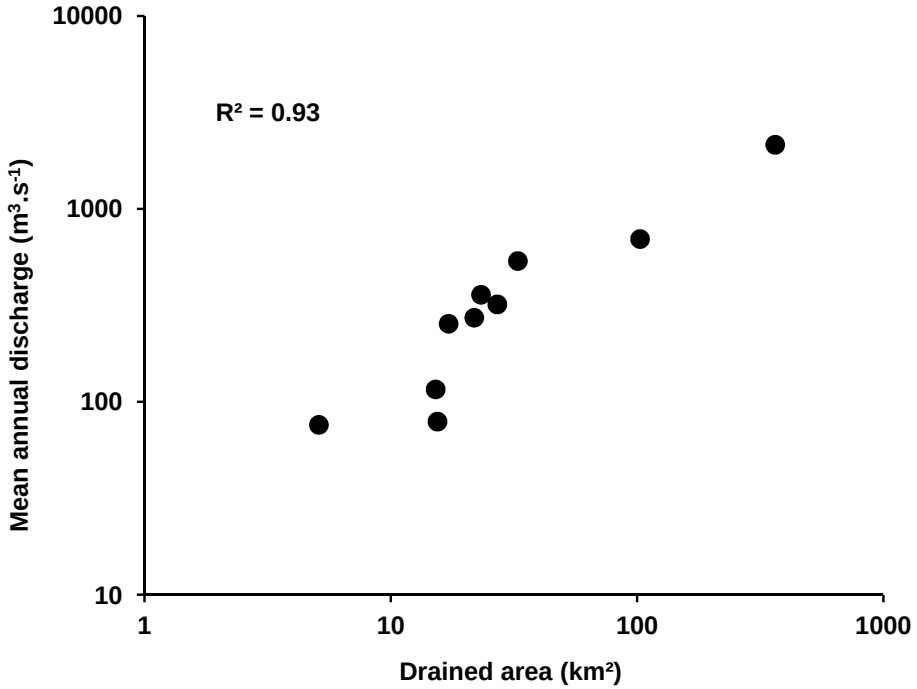

Fig. 3. Relationship between drained area and mean annual discharge in the Upper Paraguay Basin (source ANA/GEF/PNUMA/OEA, 2005).

HESSD
9, 3129–3163, 2012

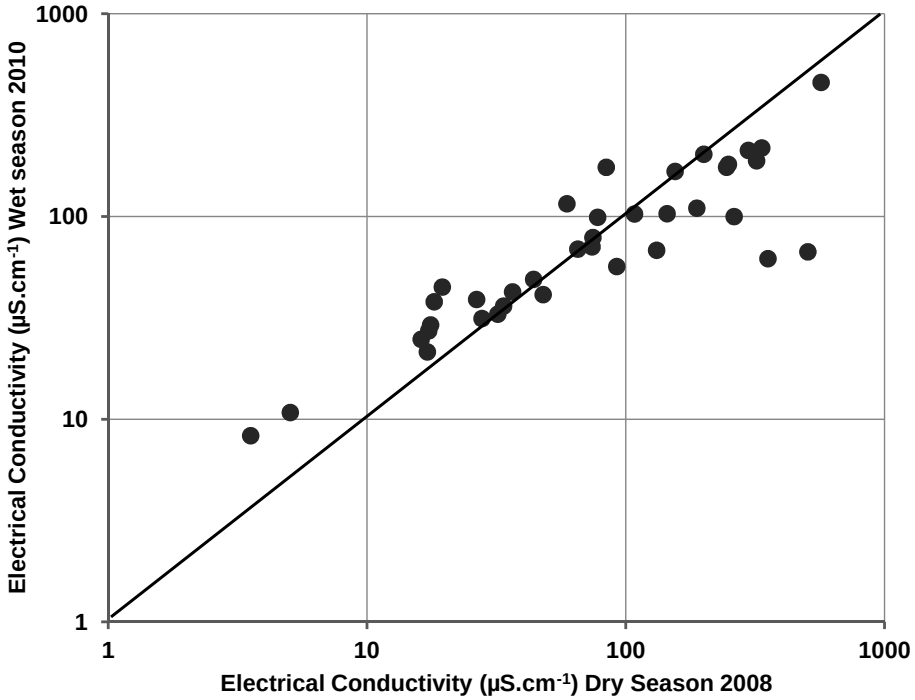

Fig. 4. Relationship between the conductivities in dry season 2008 (sampling DS) and wet season 2010 (sampling WS).

HESSD
9, 3129–3163, 2012

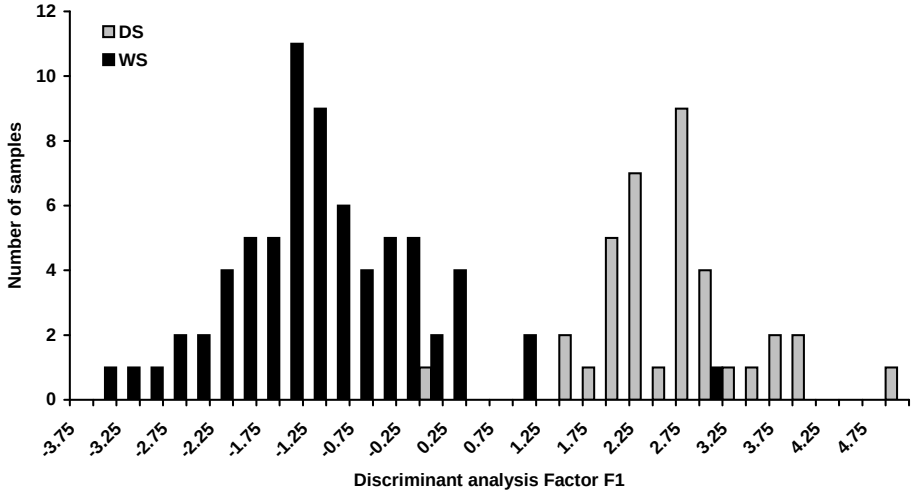

Fig. 5. Discrimination of samplings DS and WS based on major elements along factor F1.

HESSD
9, 3129–3163, 2012

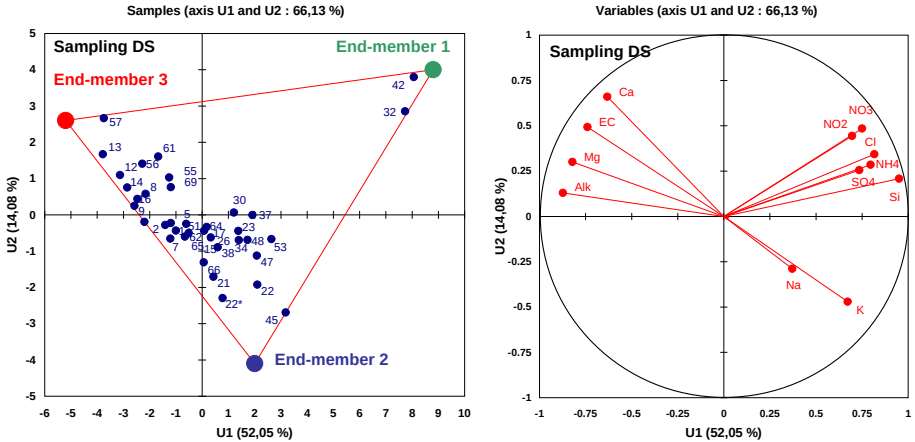

Fig. 6. Samples and variables distribution on the first factorial plan of the PCA carried out on DS sampling.

HESSD
9, 3129–3163, 2012

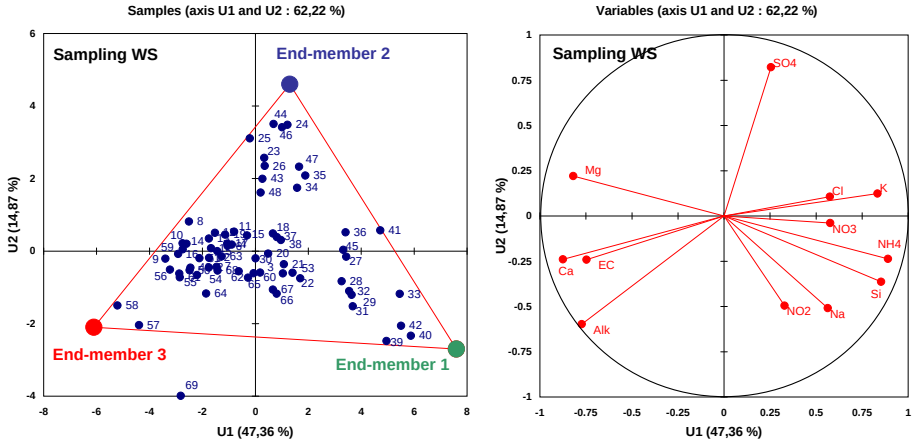

Fig. 7. Samples and variables distribution on the first factorial plan of the PCA carried out on WS sampling.

HESSD
9, 3129–3163, 2012

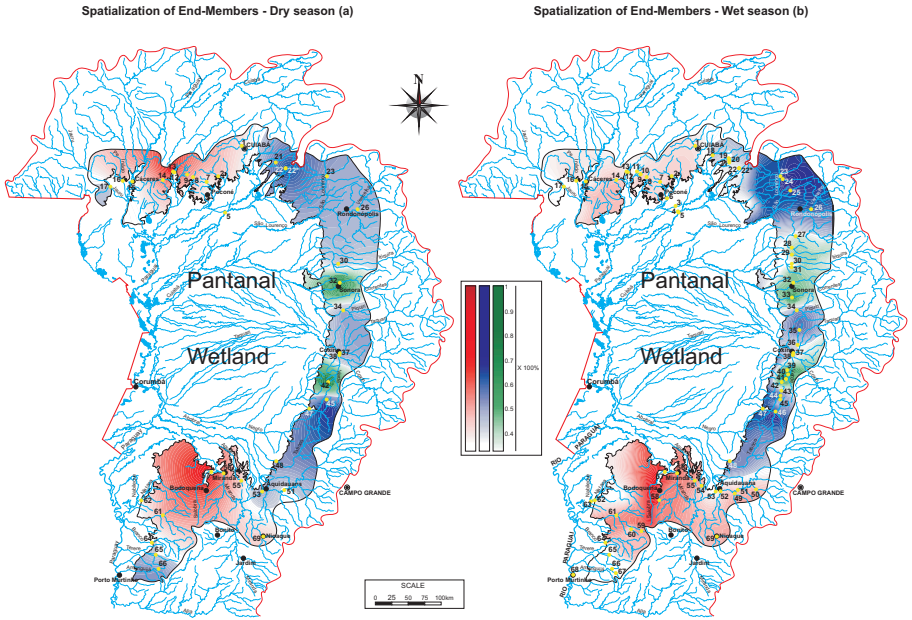

Fig. 8. Chemistry of river water at the border of the Pantanal wetland during DS 2008 **(a)** and WS 2010 **(b)**, deducted from PCA-based EMMA procedure (green: end-member 1, blue: end-member 2, red: end-member 3; contributions above 35 % are drawn).

HESSD
9, 3129–3163, 2012

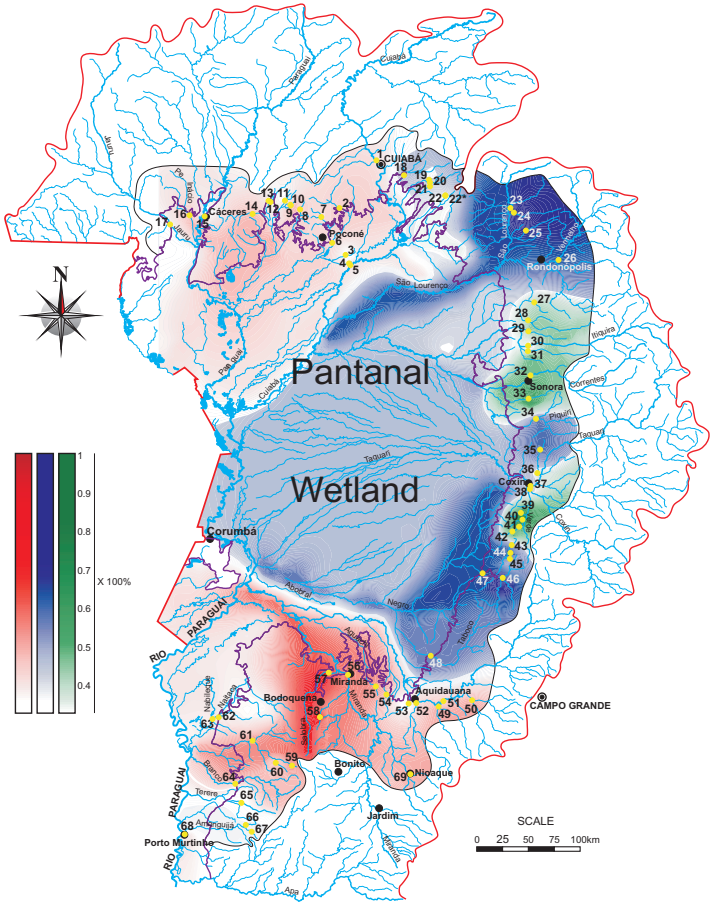

Fig. 9. Extension of the water chemistry in the Pantanal floodplain by simple tributary mixing calculation based on WS sampling (green: end-member 1, blue: end-member 2, red: end-member 3; contributions above 35 % are drawn).

HESSD
9, 3129–3163, 2012

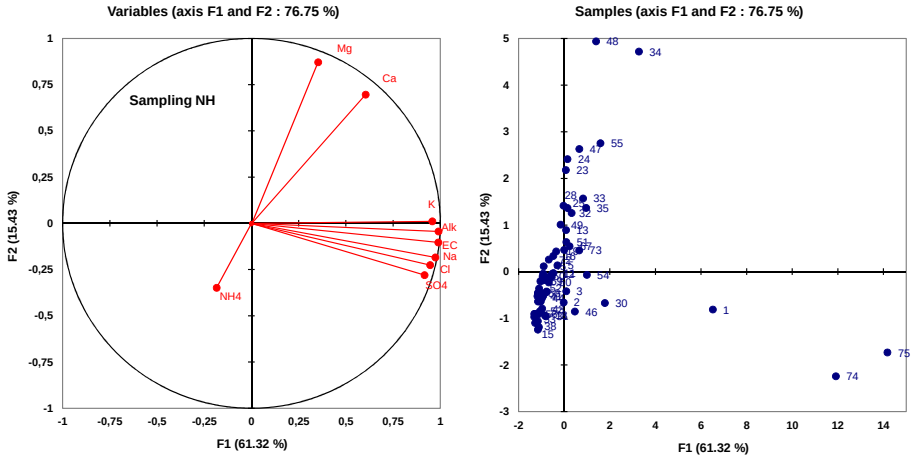

Fig. 10. First factorial plan of the PCA carried out on sampling NH.

HESSD
9, 3129–3163, 2012

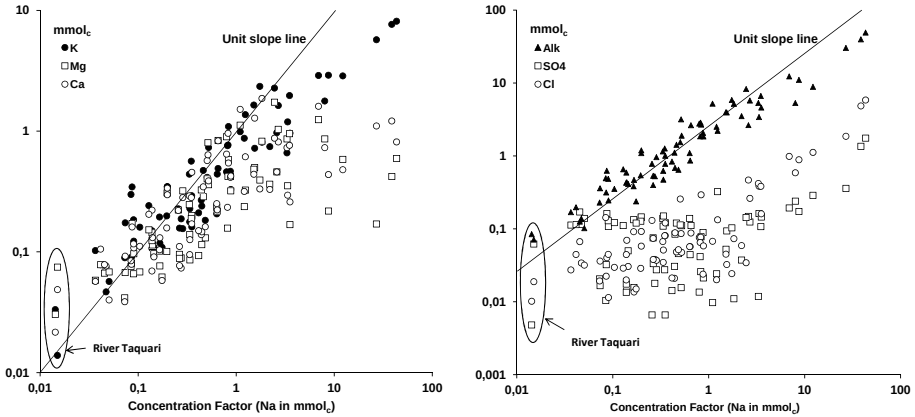

Fig. 11. Concentration diagrams for major elements of sampling NH and River Taquari (sample 37 from sampling DS and WS).

HESSD
9, 3129–3163, 2012

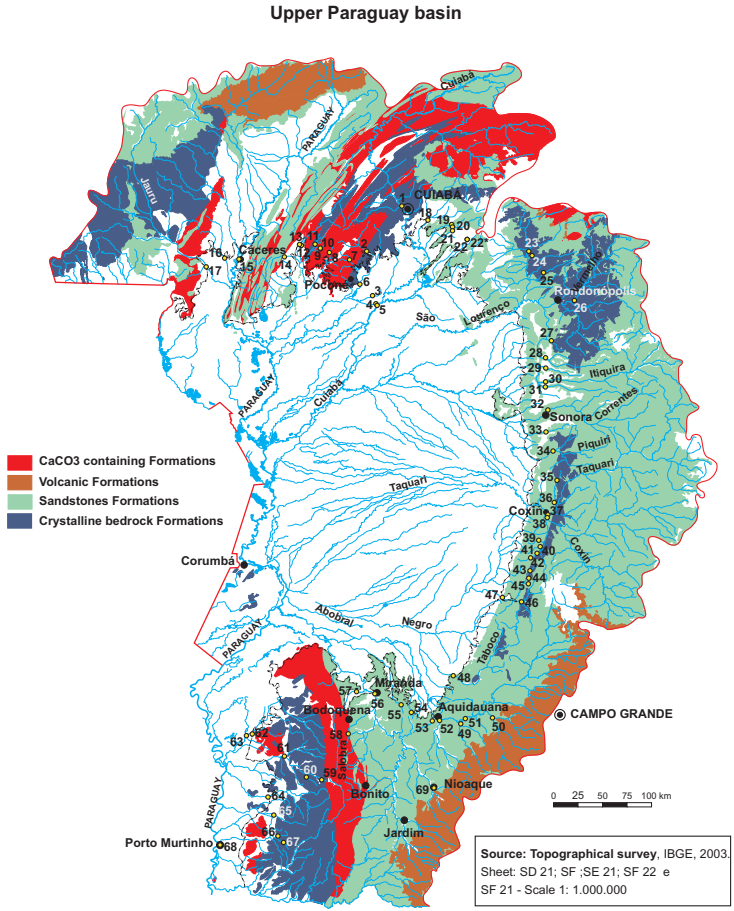

Fig. 12. Simplified map of the lithology of the Upper Paraguay Basin.

HESSD
9, 3129–3163, 2012